Cytoplasmic dynein is required to oppose the force that moves nuclei towards the hyphal tip in the filamentous ascomycete *Ashbya gossypii*

Christine Alberti-Segui, Fred Dietrich, Regula Altmann-Jöhl, Dominic Hoepfner and Peter Philippsen*

Department of Molecular Microbiology, Biozentrum, University of Basel, Klingelbergstrasse 70, CH-4056 Basel, Switzerland

*Author for correspondence (e-mail: Peter.Philippsen@unibas.ch)

Accepted 18 December 2000

Journal of Cell Science 114, 975-986 © The Company of Biologists Ltd

SUMMARY

We have followed the migration of GFP-labelled nuclei in multinucleate hyphae of *Ashbya gossypii*. For the first time we could demonstrate that the mode of long range nuclear migration consists of oscillatory movements of nuclei with, on average, higher amplitudes in the direction of the growing tip. We could also show that mitotic division proceeds at a constant rate of 0. 64 μm/minute which differs from the biphasic kinetics described for the yeast *Saccharomyces cerevisiae*. Furthermore we were able to identify the microtubule-based motor dynein as a key element in the control of long range nuclear migration. For other filamentous fungi it had already been demonstrated that inactivating mutations in dynein led to severe problems in nuclear migration, i.e. generation of long nuclei-free hyphal tips and clusters of nuclei throughout the hyphae. This phenotype supported the view that dynein is important for the movement of nuclei towards the tip. In *A. gossypii* the opposite seems to be the case. A complete deletion of the dynein heavy chain gene leads to nuclear clusters exclusively at the hyphal tips and to an essentially nucleus-free network of hyphal tubes and branches. Anucleate hyphae and branches in the vicinity of nuclear clusters show actin cables and polarized actin patches, as well as microtubules. The slow growth of this dynein null mutant could be completely reverted to wild-type-like growth in the presence of benomyl, which can be explained by the observed redistribution of nuclei in the hyphal network.

Movies available on-line:
http://www.biologists.com/JCS/movies/jcs1921.html

Key words: *Ashbya gossypii*, Cytoplasmic dynein, Nuclear distribution, Nuclear migration, Microtubules

INTRODUCTION

Nuclear migration is crucial for proper development of all eukaryotic organisms. It is an active and complex process that occurs in several important cellular events such as mitosis, fertilization or karyogamy, embryogenesis and brain development. Therefore much effort has been made to understand the mechanism of nuclear migration and to identify the components of the nuclear transport machinery.

Among eukaryotes, simple and genetically tractable fungi are powerful systems to investigate the control of nuclear movement, e.g. short range movement in yeast or long range movement in filamentous fungi. Short range nuclear migration has been extensively studied in the budding yeast *Saccharomyces cerevisiae*. Isolation of mutants with altered nuclear migration and improved video-microscopy techniques have made possible the identification of the cellular functions of the main components implicated in this process (reviewed by Hildebrandt and Hoyt, 2000). In particular, four of the seven *S. cerevisiae* microtubule (MT)-based motor proteins have been shown to be implicated in the orientation of the mitotic spindle and in nuclear movement (Meluh and Rose, 1990; Eshel et al., 1993; Li et al., 1993; Carminati and Stearns, 1997; Cottingham and Hoyt, 1997; DeZwaan et al., 1997; Saunders et al., 1997; Miller et al., 1998). For long range nuclear migration, filamentous fungi provide particularly attractive model systems (reviewed by Morris et al., 1995; Fischer, 1999). Upon hyphal extension, nuclei have to migrate towards the growing tip and to divide within the hyphae to maintain an uniform distribution of nuclei required for efficient growth of the fungal mycelium. Genetic studies in filamentous fungi have led to the identification of cytoskeletal elements, motors, and regulatory proteins implicated in nuclear migration (reviewed by Beckwith et al., 1995; Fischer, 1999). In particular, the minus-end directed MT-based motor cytoplasmic dynein has been proposed to participate actively in the process. Whereas in *S. cerevisiae* cytoplasmic dynein has an important but nonessential role in nuclear migration (Eshel et al., 1993; Li et al., 1993), it is essential for proper nuclear movement in the filamentous fungi *Aspergillus nidulans, Neurospora crassa* and *Nectria haematococca* (Xiang et al., 1994; Plamann et al., 1994; Inoue et al., 1998). In mutants lacking a functional cytoplasmic dynein heavy chain or that have mutations in genes encoding subunits of the dynein activator complex dynactin (Plamann et al., 1994; Tinsley et al., 1996; Hirozumi et al., 1999) nuclear migration is blocked or severely impaired, resulting in the formation of nuclear clusters within the hyphae. This phenotype can already be observed in developing germlings of *A. nidulans* dynein mutants where nuclei stay in the germ bubble and only migrate later, with a decreased

efficiency, into the germ tube. Altogether these observations suggest that cytoplasmic dynein provides the major motive force for nuclear movement towards the hyphal tips.

The filamentous ascomycete *Ashbya gossypii* is an attractive system to study long range nuclear transport since it is readily accessible to directed genetic alterations (Steiner et al., 1995; Wendland et al., 2000) and because of the available sequence data (F. Dietrich et al., unpublished). We have used these tools to express an in-frame histone H4-GFP fusion in *A. gossypii* hyphae which resulted in a strong fluorescent labelling of nuclei. In this paper we present in vivo studies of nuclear dynamics performed by time-lapse video microscopy that reveal an active traffic of nuclei within the growing hyphae, including continuous oscillations and frequent mitotic events. In addition to the evaluation of nuclear movements in *A. gossypii* wild-type hyphae we describe the identification of the *A. gossypii* cytoplasmic dynein as part of the major force moving nuclei away from the hyphal tip and not towards the tip as found in other filamentous fungi. We further present data showing that the tight clustering of nuclei found at hyphal tips of *A. gossypii* dynein mutant still allows formation of actively growing but nuclei-free branches with wild-type-like actin and microtubule cytoskeletons.

MATERIALS AND METHODS

Strains, media and growth conditions

Strains used in this study included *Ashbya gossypii* wild-type strain (ATCC 10895; Ashby and Nowell, 1926) and a derivative deleted for the Ag*LEU2* and Ag*THR4* genes (Altmann-Jöhl, 1996; Mohr, 1997). Strains were grown in Ashbya Full Medium (AFM medium: 1% casein peptone, 1% yeast extract, 2% glucose and 0.1% myo-inositol) at 30°C. Transformants derived from *A. gossypii* wild-type strain were selected on AFM plates containing 200 μg/ml of G418/geneticin (Gibco BRL). Transformants derived from the Ag*leu2*Δ *thr4*Δ strain were grown in Ashbya Minimal Medium (AMM medium: 1.7 g/l YNB without amino acids and ammonium sulfate, 20 g/l D(+) glucose, 0.5 g/l L-asparagine, 0.3 g/l myo-inositol), supplemented with 0.2 g/l threonine and, dependent on the experiment, with 0.03 g/l leucine. Spores were isolated from old mycelium (Wright and Philippsen, 1991) and stored in 0.025% Triton and 20% glycerol at –70°C.

Benomyl (methyl 1-[butyl-carbamoyl]-2-benz-imidazolecarbamate; M_r, 290.3; Sigma) was dissolved in DMSO at a concentration of 5 mg/ml. To test the effect of the drug on growth, 4-150 μM benomyl-containing AFM plates were prepared by adding benomyl directly into the medium before pouring the plates. To test the effect of the drug on nuclear distribution in the Ag*dhc1* null mutant, AFM liquid medium was inoculated with spores and then incubated until the cells reached a young mycelium stage (16 hours). Benomyl was then added to a final concentrations of 4-150 μM. Nocodazole (methyl-(5-[2-thienyl-carbonyl]-1H-benzimidazol-2-yl) carbamate; M_r, 301.3; Sigma) was dissolved in DMSO at a concentration of 3 mg/ml. 1-16 μM nocodazole-containing AFM plates were used to test the effect of the drug on growth.

Sequence analysis

Random sequencing of *A. gossypii* DNA clones and analysis of the predicted amino acid sequence revealed homology to *S. cerevisiae* cytoplasmic dynein heavy chain (ScDHC1) in several clones (Steiner-Lange et al., 2000; F. D., T. Gaffney, S. Goff, P. P., unpublished). Further sequencing allowed the identification of a set of overlapping clones covering the entire *A. gossypii DHC1* locus. By additional sequencing walks to fill the remaining gaps, the complete Ag*DHC1* sequence was obtained. Sequencing was performed on ABI 377 automated sequencers according to the manufacturer's instructions (PE Biosystems, Perkin Elmer CH-6343 Rotkreuz). Sequences were assembled and analysed using Phred/Phrap/Consed package (Gordon et al., 1998) and the GCG package (Womble, 2000). The final Ag*DHC1* sequence obtained in this study has been submitted to GenBank (accession number AF287477) using the Sequin form (Sequin Application Version 3.20; http://www.ncbi.nlm.nih.gov).

Construction of Ag*dhc1*-disrupted strains

Generation of the GEN3 deletion cassette carrying flanking homologies to the Ag*DHC1* gene and transformation of *A. gossypii* wild-type strain were performed according to Maeting et al. (Maeting et al., 1999) and Wendland et al. (Wendland et al., 2000). The two amplification primers S1 and S2 (see primer sequence below) were designed with 45 bp or 65 bp homology to the targeted sequence followed by 20 bp homology to the termini of the GEN3 module. The 45 bp regions of homology began 50 bp upstream of the ATG start codon (S1 primer) and 54 bp downstream of the TGA stop codon (S2 primer). This design ensures disruption of the entire Ag*DHC1* ORF. The 65 bp of homology correspond to the 45 bp of homology described above with an extension of 20 bp towards the Ag*DHC1* ORF. The analytical primers used to check the correct integration of the GEN3 marker are listed below. The *S. cerevisiae LEU2* gene with its own promoter and terminator was used as a second marker to delete the Ag*DHC1* ORF in the Ag*leu2*Δ *thr4*Δ strain. The Sc*LEU2* gene has been shown to be functional in *A. gossypii* (Mohr, 1997). The pScLEU2 plasmid used as a template to generate the ScLEU2 deletion cassette was created by insertion of the entire Sc*LEU2* gene between the *Bgl*II site of pAF100 (Thierry et al., 1990). Since pGEN3 and pScLEU2 share the same vector backbone, we used the same S1 and S2 primer pair to generate a ScLEU2 cassette with flanking homology to the Ag*DHC1* gene. Preparation of the PCR fragments and transformation of Ag*leu2*Δ *thr4*Δ strain were performed according to the protocol described by Wendland et al. (Wendland et al., 2000) with some modifications as described below. After electroporation, the mycelium was resuspended in 6 ml AMM liquid medium containing 0.2 g/l threonine and 0.03 g/l leucine and incubated for 8 hours at 30°C to allow expression of the Sc*LEU2* marker. Then the mycelium was washed in sterilized water and spread on AMM plates containing no leucine. Transformants were detected after 4 days of incubation at 30°C. Analytical primers used to check the correct integration of the ScLEU2 marker were identical to those used for the GEN3 marker.

Primer List: (homologies to the GEN3 marker are written in lower case letters)

S1 primer (45 bp): 5′CAGACTAAGATCGCAGAACGGCATTGGAAGGGCAAACACGGGAGCgctagggataacagggtaat 3′

S1 primer (65 bp): 5′CAGACTAAGATCGCAGAACGGCATTGGAAGGGCAAACACGGGAGCTGAAGATGACCGATGATCAGgctagggataacagggtaat 3′

S2 primer (45 bp): 5′CTAACATACAAAAAAGCAAAAGACTGGTGAGTACTGGAGGTATGGaggcatgcaagcttagatct 3′

S2 primer (65 bp): 5′CTAACATACAAAAAAGCAAAAGACTGGTGAGTACTGGAGGTATGGACATTACACTCAGTGAATTAaggcatgcaagcttagatct 3′

G1 primer: 5′GACCAGAGCGAGGCCACG 3′

G4 primer: 5′GTCGCTATTCAGTACATAGTC 3′

I1 primer: 5′GATCGACTCCTGCTTCGCC3′

I2 primer: 5′CGAGTTGGCACGACTCCG 3′

G2 primer: 5′GTTTAGTCTGACCATCTCATCTG 3′

G3 primer: 5′TCGCAGACCGATACCAGGATC 3′

Fluorescence microscopy of fixed cells

For visualization of nuclei, cells were stained with 4′,6-diamidino-2-phenylindole (DAPI). Fixation and staining of the specimen were performed as follows. Cells were grown in AFM liquid medium to

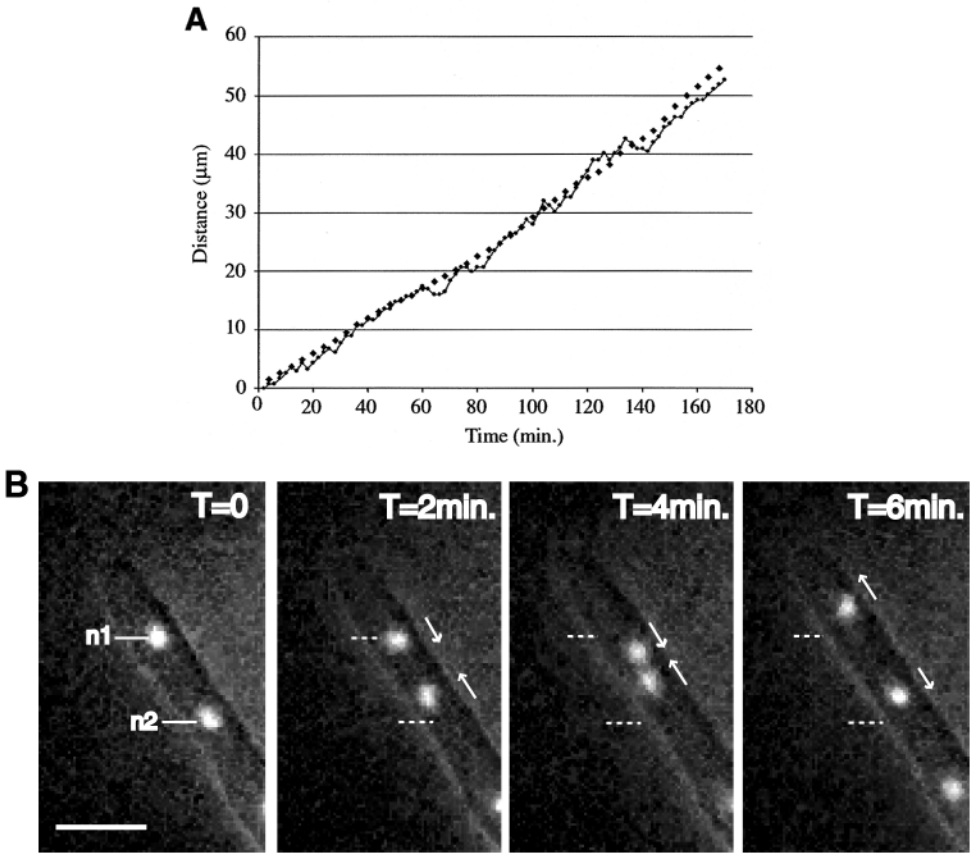

Fig. 1. In vivo study of nuclear migration in *A. gossypii* wild-type hyphae. (A) Graphical representation of the distance in μm migrated by a leading nucleus within 3 hours. During that time the nucleus did not undergo mitosis. The dots depict the movement of the leading nucleus. The distance was measured between the initial position of the nuclear center at T=0 and its current position at T=*n*. The diamonds represent the hyphal tip extension. The distance was measured between the initial position of the hyphal tip at T=0 and its current position at T=*n*. According to the slopes of both curves, the average speed of the nucleus and the hyphal tip extension are 0.3 μm/minute. (B) Oscillations of nuclei during hyphal tip extension. Histone H4-GFP-labelled nuclei were observed by time lapse video microscopy as described in Materials and Methods. n1 and n2 indicate the leading (or first) nucleus and the second nucleus, respectively. The dashed lines at T=2, 4, 6 minutes mark the initial positions of n1 and n2 at T=0. The apparent direction of nuclear movement is indicated by arrows. At T=2 minutes and T=4 minutes, both nuclei have moved closer to each other. At T=6 minutes, they are further apart. This short series of four pictures is derived from a movie taken over a period of 7 hours (see movie1). Bar represents 8 μm. (See movie 1, http://www.biologists.com/JCS/movies/jcs1921.html)

early log phase and collected by a short centrifugation at 3000 rpm in a table top centrifuge. Four volumes of 70% ethanol supplemented with 1 μg/ml DAPI were added to one volume of cells. An incubation of 2 minutes was sufficient to allow fixation and penetration of the fluorescent dye into the specimen. Cells were then washed once with sterilized water and mounted on a slide for microscopic observations. Pictures were taken on an axioscope microscope (Carl Zeiss AG, Feldbach, Switzerland) equipped with a VI-470 camera and a LG-3 scientific frame grabber (PCI version). Cells were visualized using a Plan-Neofluar 100× oil objective and illuminated with UV light to view the DAPI staining (filter set 02; Carl Zeiss AG, Feldbach, Switzerland). Images were captured using NIH Image (developed at the US National Institutes of Health http://rsb.info.nih.gov/nih-image/) and processed in Photoshop 4.0 (Adobe Systems Europe Ltd., Edinburgh, GB).

Microtubules were immunostained according to the following protocol: fresh spores were suspended in AFM liquid medium to a concentration of 1×5.10^4 and grown overnight at 30°C. For fixation, 100 μl of young mycelia were rapidly washed with 1 ml of freshly prepared fixation buffer (3.7% formaldehyde in 0.1 M KPO_4 pH 6.5, 1 M sorbitol), resuspended in 1 ml fixative, and incubated 1 hour at room temperature with occasional shaking. Cells were then washed four times with 1 ml washing buffer B1 (0.1 M potassium phosphate, pH 6.5, 1 M sorbitol), once with 1 ml washing buffer B2 (1.2 M sorbitol/0.1 M phosphate citrate pH 5.9) and finally resuspended in 200 μl of buffer B2. For partial digestion of the fungal cell wall, cells were incubated 1 hour at 30°C in the presence of 1.8 μl of 25 mg/ml Zymolyase 20T (Seikagaku corporation, Japan). Cells were then washed once with 1 ml buffer B2 and resuspended in a final volume of 100 μl. For immunostaining, 5 μl of cells were mounted on an 8-well Flow Labs slide previously coated with 1 mg/ml poly-L-lysine (M_r 400×10^3; Sigma). The slide was then plunged into methanol precooled to –20°C for 5 minutes and transferred into acetone at –20°C for 20 seconds. The slide was left at room temperature to evaporate the acetone and then placed on the top of a moist tissue. Samples were then immersed in the respective primary antibody for 1 hour in the dark at room temperature. Following three washes in 1% BSA-PBS (0.04 M K_2HPO_4, 0.01 M KH_2PO_4, 0.15 M NaCl, 1 mg/ml NaN_3) the cells were immersed in the appropriate secondary antibody for 1 hour. The secondary antibody was washed 6 times with 1% BSA-PBS. Samples were subsequently mounted in pd-DAPI (100 mg p-phenylenediamine pH 8 dissolved in 10 ml PBS, 50 ng/ml DAPI, 90 ml glycerol). Pictures were taken on an Axioplan 2 microscope (Carl Zeiss AG, Feldbach, Switzerland) equipped with a Plan-Neofluar 100×/1.3 oil PH3 objective and a TE/CCD-1000PB back-illuminated cooled CCD camera. As an epifluorescence illumination source, a mercury arc lamp was used. Thirty z-axis plane fluorescent images were acquired and processed using Metamorph Software version 3.5.1 (Universal imaging). In this study, monoclonal anti-β-tubulin mouse IgG antibodies (Boehringer) were used as primary antibodies at a 1:50 dilution. Donkey anti-mouse IgG conjugated to Cy3, provided by R. Sütterlin (Biozentrum, University of Basel, Switzerland), were used as secondary antibodies. Cy3 was observed using filter set 15 (Carl Zeiss AG, Feldbach, Switzerland). To visualize nuclei, filter set 02 was used.

For visualization of the actin cytoskeleton, cells in early log phase were fixed in 3.7% formaldehyde and 0.2% Triton X-100 for 10 minutes at room temperature, rinsed 2 times in PBS and resuspended in 100 μl PBS. 1 μl of 50 μM Alexa stock solution (Molecular Probes) was added and the suspension was incubated 90 minutes in the dark

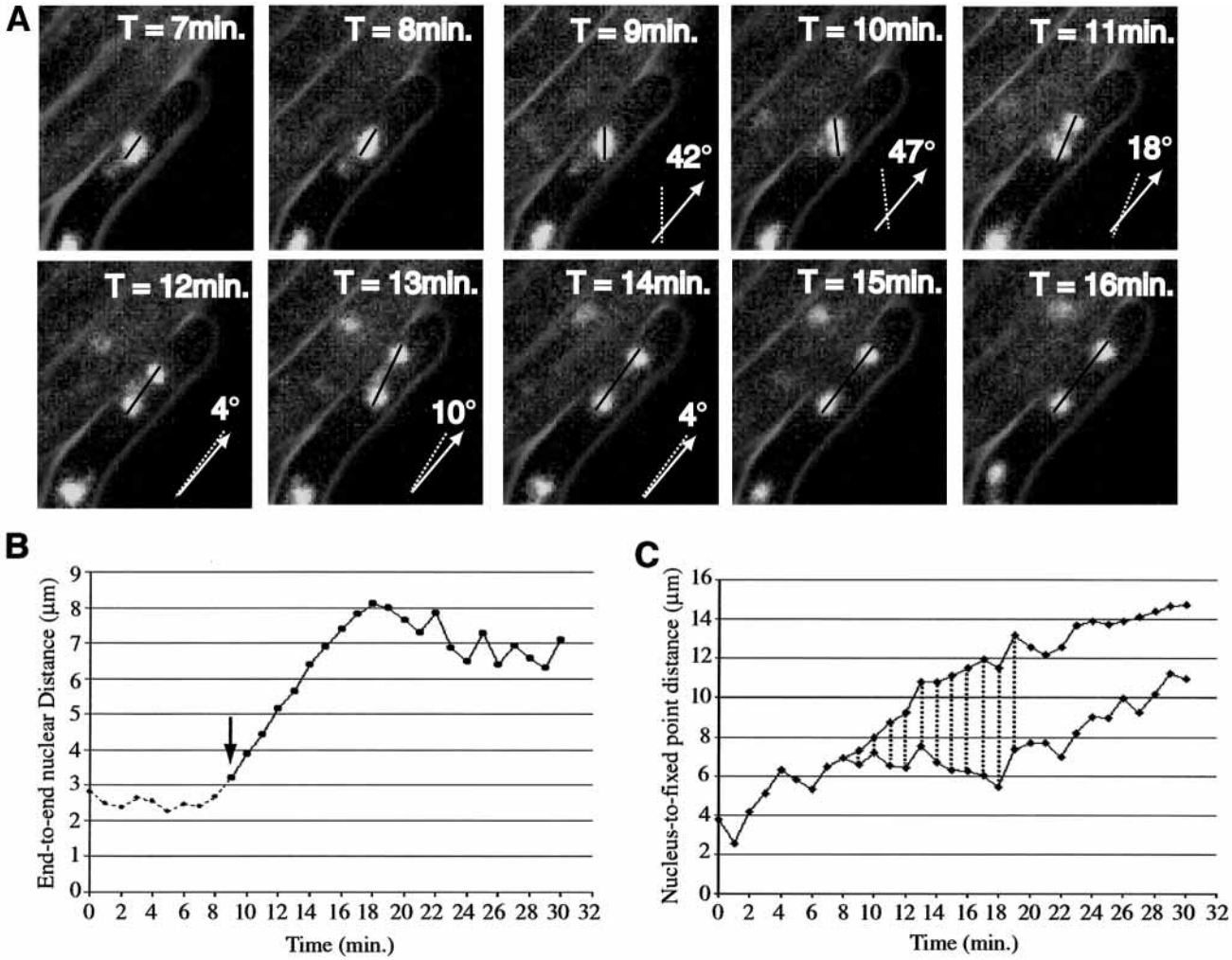

Fig. 2. Mitosis as observed in hyphae carrying GFP-labelled nuclei. (A) Kinetics of nuclear division. The ten pictures are taken from a series of 30 images collected at 1-minute intervals. Prior to division the leading nucleus oscillates and changes in shape (T=0 to T=8 minutes). The nucleus starts to elongate at T=9 minutes. Two clearly separated chromosomal masses are visualized at T=11 minutes. The angle between the axis of nuclear elongation (dotted line) and the axis of growth (white arrow) is indicated for time points T=9 to T=14. B. Monophasic nuclear division. Distances between nuclear ends (represented as black bars in the picture series) were plotted as a function of time. The first part of the graph (thin dotted line) represents changes in shape of the interphase/metaphase nucleus. The second part (plain line) depicts the variation in end-to-end distances between the two chromosomal masses. The arrow indicates the visual start of elongation. (C) Oscillations of dividing nuclei. The distances between a fixed point and the nuclear centers were plotted against time. The dotted lines between the two curves represent the increasing distance between the centers of the two chromosomal masses.

at room temperature (P. Knechtle, personal communication). Three minutes before the end of the incubation, 0.4 µl of 1 mg/ml DAPI stock solution was added to allow subsequent visualization of nuclei. Cells were then washed 5 times in PBS and mounted in pd-DAPI. The equipment used to take pictures of actin was identical to the one used to visualize microtubules except that filter set 10 (Carl Zeiss AG, Feldbach, Switzerland) was selected.

In vivo time lapse video microscopy

Construction of pAG-H4-GFP-KanMX6

C-terminal fusion of the S65T variant of GFP (Heim et al., 1995) to the *A. gossypii* histone H4 was performed by co-transformation in *S. cerevisiae* of a pAG clone carrying the entire *Ashbya* H4 gene and a PCR cassette consisting of the GFP-KanMX6 double module (Wach et al., 1997). The PCR cassette was flanked by 45 bp of homology to sequences upstream and downstream of the 3′ end of the histone H4 gene. The pAG clone used in this study was derived from a plasmid library constructed by Ch. Mohr by cloning partial Sau3A-cleaved genomic *A. gossypii* DNA into pRS416 (Mohr, 1997; Sikorski and Hieter, 1989). The yeast pFA-6b-S65TGFP-KanMX6 plasmid was used to generate the PCR module as previously described (Wach et al., 1997). The resulting pAG-H4-GFP-KanMX6 plasmid was introduced into *A. gossypii* wild-type strain by standard transformation procedures. This plasmid carries a *S. cerevisiae* ARS element and is able to replicate in *A. gossypii* (Wright and Philippsen, 1991). Spores were isolated from primary transformants and grown in the presence of 200 µg/ml G418. Spores carrying the pAG-H4-GFP-KanMX6 plasmid were able to germinate and to develop into young mycelia containing fluorescent nuclei.

For in vivo time lapse studies, spores were grown 16 hours at 30°C in AFM liquid medium. The specimen was then placed on the top of the agarose surface of a ground-well microscopy slide as previously described (Hoepfner et al., 2000). For growth, we used AFM medium diluted 4 times combined with 1% agarose.

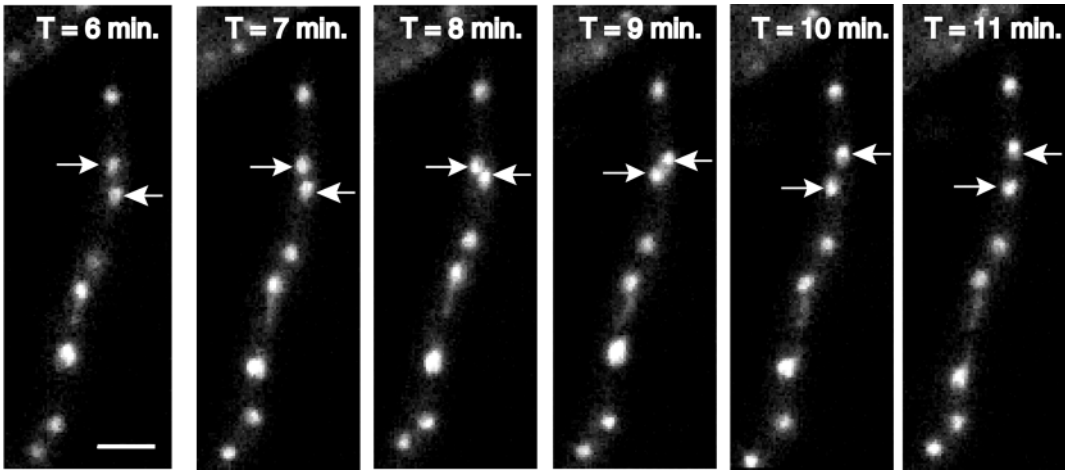

Fig. 3. By-passing of nuclei as observed in hyphae carrying GFP-labelled nuclei. The straight white arrows indicate the by-passing of two daughter nuclei. Bars represent 6 μm. This series of pictures is taken from movie 2 (http://www.biologists.com/JCS/movies/jcs1921.html).

Video microscopy, image acquisition and picture processing

The microscope set-up used in this study was identical to the one described previously (Hoepfner et al., 2000). The filter set 17 (Carl Zeiss AG, Feldbach, Switzerland) was used to visualize nuclei. The H4-GFP acquisition settings were 1 or 2 minute intervals, 0.1 second exposure time, 12% transmission illumination and one z-axis plane. The temperature on the microscope slide was approx. 25°C. Using these conditions cells showed steady growth for over 10 hours. Image acquisition using Metamorph and movie processing using Adobe Premiere were performed as previously described (Hoepfner et al., 2000).

RESULTS

In vivo study of long range nuclear migration in *A. gossypii* wild-type hyphae

A. gossypii wild-type hyphae, like hyphae of other filamentous ascomycetes, consist of a succession of multinucleate compartments delimited by septa (Wendland and Philippsen, 2000; Ayad-Durieux et al., 2000). For the in vivo study of nuclear migration, we performed time lapse video microscopy of hyphae carrying GFP-labelled nuclei (see Materials and Methods). Under time-lapse conditions, the hyphae grew for at least 10 hours with a tip growth rate of 0. 3 μm per minute. Upon hyphal extension we observed a general movement of nuclei towards the growing tip with a migration rate for the leading nucleus similar to the hyphal tip extension (0.3±0.1 μm/minute; see Fig. 1A). However, the nuclear movement did not occur unidirectionally towards the growing tip. Nuclei were constantly oscillating back and forth. Adjacent nuclei were frequently getting close to each other or were rapidly moving away from each other (Fig. 1B). In addition, the oscillating nuclei often appeared stretched, resulting in an elongated structure. We estimated the velocity for such oscillations to occur in the range of 0.5-2 μm/minute and occasionally even 5 μm/minute. Nuclear oscillations were abolished in the presence of 8 μM nocodazole, a microtubule (MT)-destabilizing drug (see movie 3: http://www.biologists.com/JCS/movies/jcs1921.html). This indicates that these short range and irregular back and forth movements are dependent on an intact microtubule network.

A resolution time of one picture every minute allowed us to capture mitotic events. Mitoses were frequently observed in the hyphal tip compartments. Despite the presence of up to six nuclei in these compartments, we did not observe more than two nuclei undergoing mitosis synchronously. Often only a single nucleus underwent mitosis. One example out of seven mitotic events that were observed in detail is shown in Fig. 2A together with two modes of quantitative evaluations (Fig. 2B,C). First, nuclear division was tracked by measuring, every minute, the distance between the ends of the dividing nuclear masses. The actual numbers obtained for the particular mitotic event of Fig. 2A are presented in Fig. 2B. Measurements from all seven mitoses revealed that prior to division the nuclear end-to-end distance was 2.23 μm (s.d.=0.21; n=48). Separation of the two chromosomal masses occurred at a constant rate of 0.64 μm/minute (s.d.=0.08; n=7). A maximal end-to-end distance of 8-9 μm was reached 9-10 minutes after the starting point of elongation. Shortening of the end-to-end distance started thereafter (see example in Fig. 2B) most likely indicating breakdown of the mitotic spindle. The irregular changes in the end-to-end distances measured during the following period were consistent with the observed independent oscillations of interphase nuclei (see Fig. 1). Second, the distance between the center of the two chromosomal masses and a fixed point was plotted against time (Fig. 2C). Nuclei were oscillating prior, during and after division. The synchronous back and forth movement of the two DNA masses during the 9 minutes of linear elongation indicated that during that period they were interconnected. Independent oscillatory movements of the two chromosomal masses were recorded just after the maximal elongation (6 μm center-to-center distance).

For all seven mitoses the early elongation occurred obliquely (15-80°) to the axis of growth, followed by a repositioning along this axis later in mitosis as indicated in Fig. 2A. Occasionally, mitosis in *A. gossypii* wild-type hyphae was followed by the by-passing of daughter nuclei (Fig. 3; see also movie 2). Nuclear by-passing was also observed among interphase nuclei close to or more distant from hyphal tips (data not shown). In rare cases one nucleus was seen to by-pass several nuclei. In addition, migration of nuclei through septa, as seen in other filamentous ascomycetes, was frequently observed, sometimes followed by a back movement to the original compartment (data not shown). The coordination of these different forms of nuclear dynamics (oscillations,

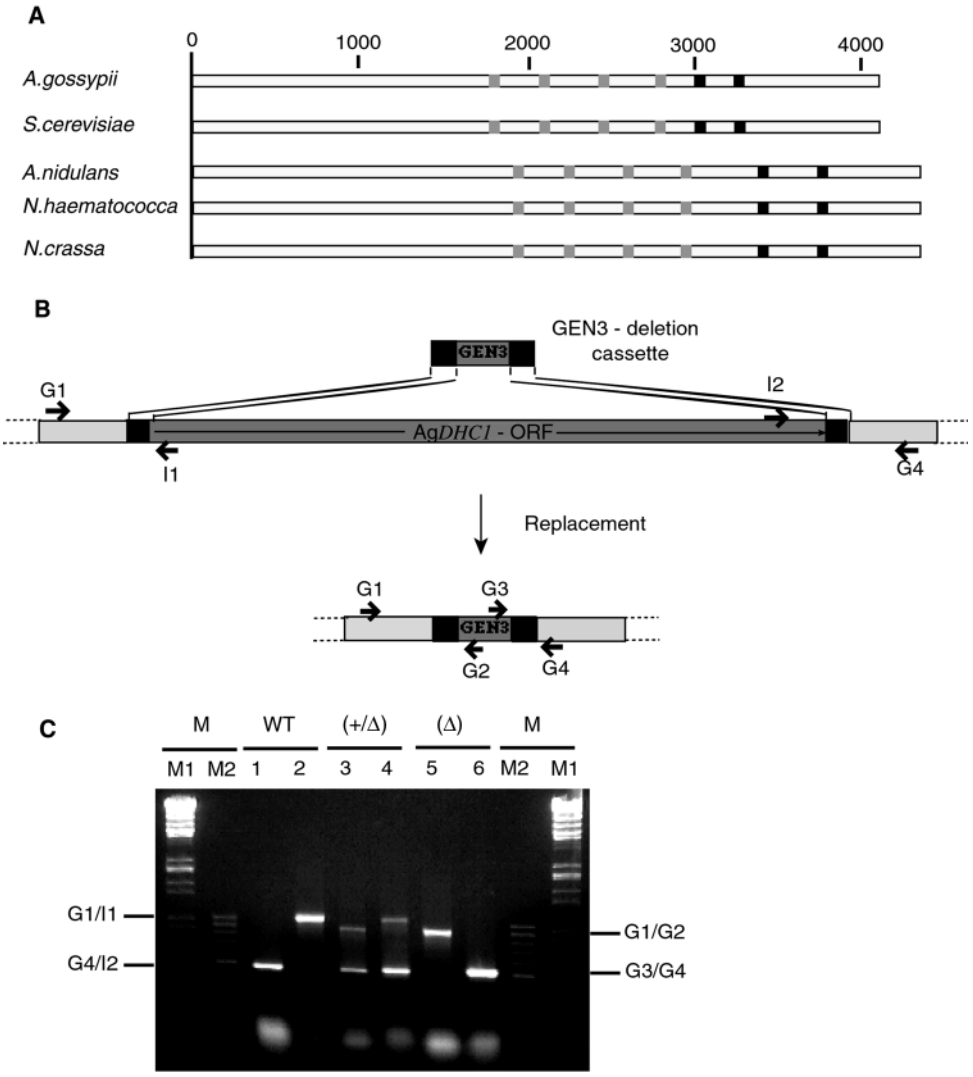

Fig. 4. Domain composition of AgDHC1 and generation of strains lacking AgDHC1. (A) Schematic representation of fungal cytosolic dynein heavy chains. The *A. gossypii* DHC1 protein (4083 aa) is represented together with *S. cerevisiae* (4092 aa; Swissprot accession number P36022) *N. crassa* (4367 aa; Swissprot accession number P45443), *N. haematococca* (4349 aa; Swissprot accession number P78716) and *A. nidulans* (4344 aa; Swissprot accession number P45444) dynein heavy chains. The gray boxes mark the position of the four P-loops and the black boxes indicate the two predicted coiled-coil regions. (B) Deletion of the entire Ag*DHC1*-ORF. The Ag*DHC1* locus is shown before and after integration of the GEN3-deletion cassette. Analytical primers are indicated by small arrows and positioned according to the sequences they are homologous to. (C) Verification PCR on heterokaryotic (+/Δ) and homokaryotic (Δ) transformants, including *A. gossypii* wild type (WT) as a control. Two different combinations of three primers were used: G1/G2/I1 (lane 1, 3, 5) and G4/G3/I2 (lane 2, 4, 6). I1 and I2 are internal primers that were used to indicate the presence of the Ag*DHC1* gene. No G1/I1 or G4/I2 PCR products were obtained in the homokaryotic transformants indicating that the Ag*DHC1* ORF has been deleted. PCR products were loaded on a 1.2% agarose gel. M: DNA size markers (M1: λ *Hin*dIII + *Hin*dIII/*Eco*RI digest; M2: DNA size marker 100-1000 bp – BioLadderTM 100).

mitosis, by-passing of nuclei and movement through septa) with growth results in a more or less uniform nuclear distribution with an average distance between nuclei of 6.65 μm (s.d.=1.35; *n*=168).

Characterization of the Ag*DHC1* gene

Preliminary experiments with targeted deletions of *A. gossypii* genes encoding putative MT-based motor proteins showed a strong nuclear migration defect only for deletions in the dynein heavy chain gene Ag*DHC1* (Altmann-Jöhl, 1996; C. A.-S., unpublished). The complete Ag*DHC1* sequence was obtained as described in Materials and Methods. The ORF is 12.2 kb long, containing no intron and encoding a predicted polypeptide of 4083 amino acids. AgDHC1 is similar in length to *S. cerevisiae* dynein heavy chain (ScDHC1; 4092 aa) but substantially shorter when compared to the cytoplasmic dynein heavy chains of the filamentous ascomycetes *N. crassa* (4367 aa), *N. haematococca* (4349 aa) and *A. nidulans* (4344 aa). Multiple sequence alignment of the five dynein motors revealed the absence in AgDHC1 as well as in ScDHC1 of amino acid stretches of various length (2 to 35 residues) over the entire protein. The predicted amino acid sequence of AgDHC1 shares 39% identity with ScDHC1 and 34% identity with *A. nidulans*, *N. haematococca* and *N. crassa* DHCs which is significantly lower than the 70% identity found when these three filamentous fungal DHCs are compared with each other. In particular, from the over thirty highly conserved blocks present in the first 1900 amino acids of *A. nidulans*, *N. haematococca* and *N. crassa* DHCs, only five are found in the amino terminus of AgDHC1. This points to a substantial difference in the presumptive cargo binding region of AgDHC1 compared to the other three filamentous ascomycetes. A higher degree of homology is found in the motor domains characterized by the four regularly spaced ATP binding sites (P-loops) followed by the two coiled-coil regions (Fig. 4A). According to recent findings (Gee et al., 1997; Koonce, 1997; Koonce and Tikhonenko, 2000), these two coiled-coil regions are involved in the formation of a stalk that emerges from the globular motor domain allowing binding to microtubules.

Generation of Ag*dhc1* null mutants

A one step PCR-based gene targeting approach (Wendland et al., 2000) was used to delete the complete Ag*DHC1* ORF. In the attempt to remove this 12.2 kb DNA fragment, we

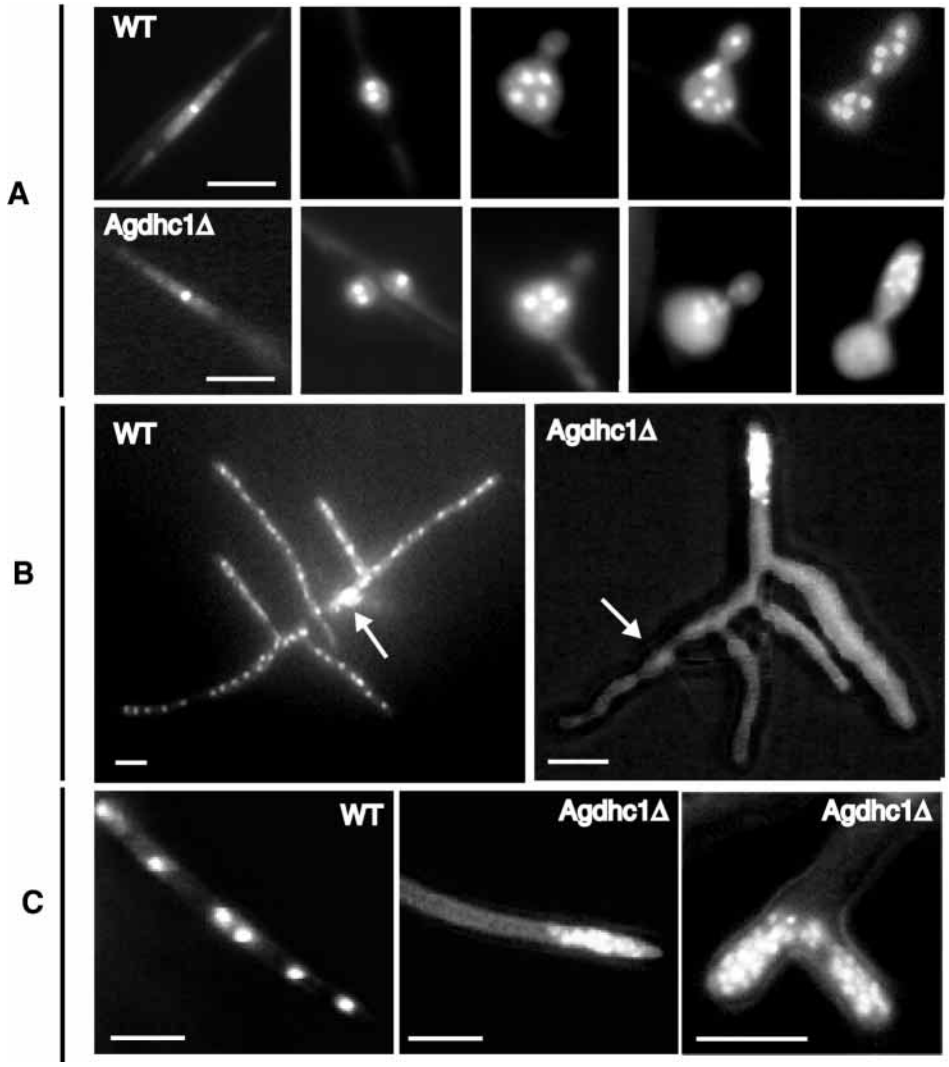

Fig. 5. Effect of the dynein heavy chain deletion on nuclear distribution.
(A) DAPI staining of germinating *A. gossypii* spores. Wild-type spores (upper panels) and Ag*dhc1*Δ spores (lower panels) were allowed to germinate in AFM liquid medium. The left panels show non-germinated spores, and the four right panels, germination stages between 7 and 9 hours. The only apparent difference between the two developmental patterns is seen when nuclei start migrating out of the germ bubble into the germ tube.
(B) Nuclear distribution in young wild-type and Ag*dhc1*Δ mycelia. The arrows indicate the position of the needle shaped spore which usually develops two germ tubes in opposite orientations. Note that nuclei in the Ag*dhc1* null mutant are in prominent clusters at one hyphal tip leaving behind anucleated hyphae including branches.
(C) Examples of DAPI staining of hyphal tips of old mycelium. Bars represent 10 μm.

generated a deletion cassette with short guide sequences of either 45 bp or 65 bp of homology to sequences upstream and downstream of the targeted Ag*DHC1* ORF (Fig. 4B). Ten transformants were obtained with the cassette containing the 45 bp homology regions and twice as many with the longer homology regions. Five of these heterokaryotic transformants were picked and used for verification analysis and for isolation of homokaryotic spores. To verify the correct integration of the cassette, an analytical PCR was performed using a set of six different primers. The positions of these verification primers are shown in Fig. 4B. All tested transformants showed correct gene replacement. Examples of this verification analysis are documented in Fig. 4C. Whereas in the heterokaryotic mycelium both wild-type and recombinant alleles were detected, only the deletion allele was found in the homokaryotic mycelium. This confirms the complete deletion of the Ag*DHC1* ORF. Dynein null mutants were also generated using the ScLEU2 marker (see Materials and Methods) and were similarly checked by PCR (data not shown).

Growth and colony morphology of *Agdhc1* null mutants

Because homokaryotic Ag*dhc1*Δ strains lost the ability to sporulate, all following assays were performed with spores isolated from heterokaryotic mycelium by micromanipulation and subsequent growth on AFM medium containing 200 μg/ml geneticin. Similar to wild-type spores, *Agdhc1* null mutants were able to germinate after around 7 hours of incubation at 30°C. When observed by microscopy, the initial stages of development, germ bubble and bipolar germ tube formation, proceeded without any apparent morphological defect such as hyphal swelling or hyphal contortion. A reduction in growth as well as a change in hyphal morphology were noticed during germ tube elongation and formation of the young branched Ag*dhc1*Δ mycelium. After several days incubation at 30°C, *Agdhc1* null mutants only succeeded in forming a very small and compact colony that clearly differed from the large and well-spread wild-type colony (see below). The drastic drop in growth rate was observed for each of the independent transformants analysed. Analysis of the colony diameter after 5 days incubation at 30°C on AFM full medium, indicated that the radial growth rate of the *Agdhc1* mutant is only 14±2% (n=50) of that of the wild type. Upon prolonged incubation for up to 20 days no fast growing sectors appeared.

In conclusion, disruption of the dynein motor in *A. gossypii*

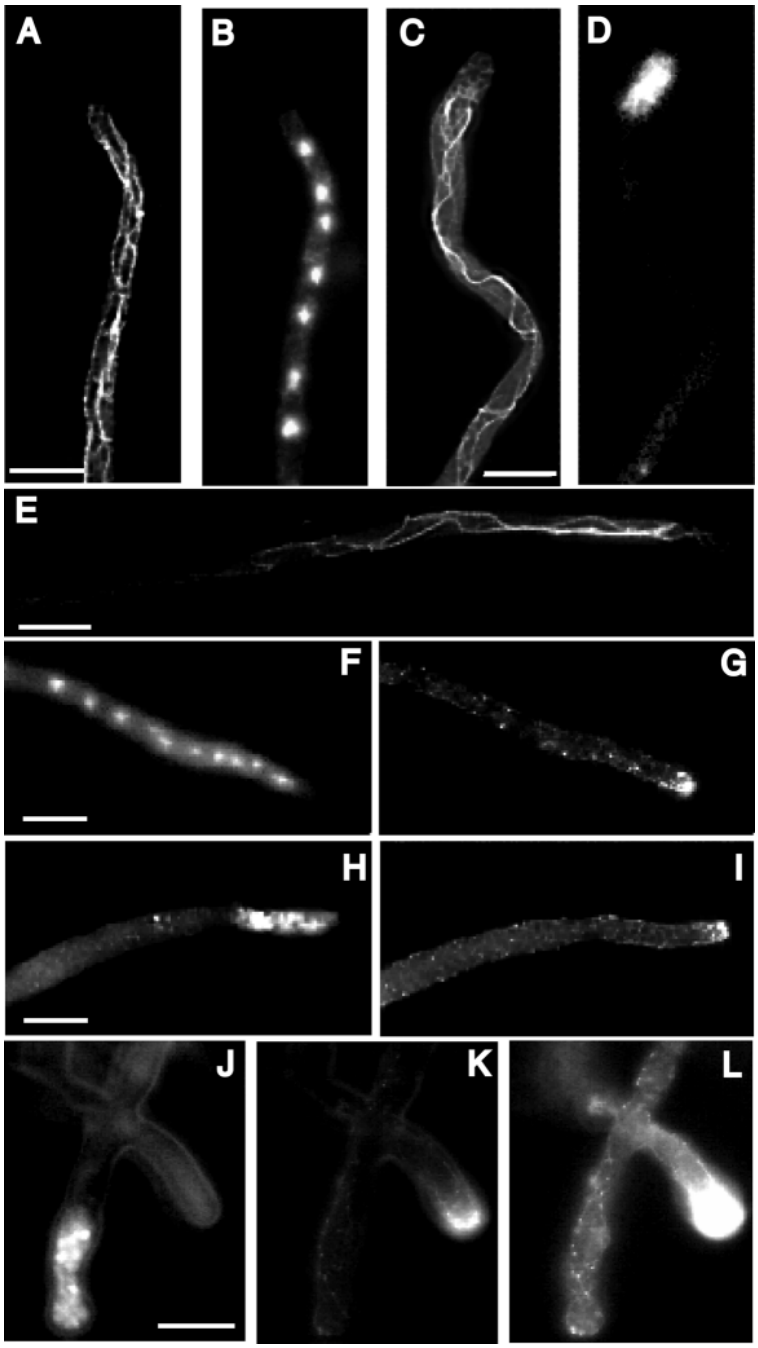

Fig. 6. Visualization of microtubules and actin cytoskeleton together with nuclei in wild-type and Ag*dhc1* null mutant. (A-D) Cytoplasmic microtubules and nuclei in one hyphal tip compartment of *A. gossypii* wild-type mycelia (A,B) and in one hyphal tip compartment of Ag*dhc1* null mutant (C-D). (E) Maximal length of cytoplasmic microtubules in Ag*dhc1*Δ hyphae; the tip with the nuclear cluster is located at the extreme right end of this panel. (F-I) Nuclei and actin cytoskeleton in one hyphal tip compartment of *A. gossypii* wild-type mycelia (F,G) and in one hyphal tip compartment of Ag*dhc1* null mutant (H,I). (J-L) Nuclear cluster (J) and actin cytoskeleton (K,L) in one hyphal tip with adjacent branch, of Ag*dhc1* null mutant. L is an overexposure of the image in K. Microtubules were visualized by immunofluorescence (A,C,E), actin was stained with rhodamine-phalloidine (G,I,K,L) and nuclei with DAPI (B,D,F,H). For microtubule and actin pictures, 30 z-axis fluorescent image planes, spaced at 0.5 μm intervals along the z-axis, were averaged and merged using the metamorph software. Bars represent 10 μm.

severely affects fungal growth but does not result in a lethal phenotype.

Nuclear distribution in Ag*dhc1* null mutants

During the first phase of development, the nuclear distribution pattern of germinating Ag*dhc1*Δ spores is very similar to that of the wild type. Clear differences are observed when nuclei start moving out of the germ bubble into the germ tube (Fig. 5A). Instead of a progressive nuclear migration as observed in the wild type, in the Ag*dhc1* null mutant all nuclei start migrating together towards the growing tip. This leads to an extremely biased nuclear distribution in the Ag*dhc1*Δ young mycelium compared to wild type, as documented in Fig. 5B. For each of the 100 young Ag*dhc1*Δ mycelia that were analysed by DAPI staining, all nuclei were located as single cluster at only one hyphal tip. This indicates that the nuclear cluster formed in the germling is maintained at the tip and moves together with the growing apex, leaving behind nuclei-free hyphal compartments. In hyphae of older mycelia nuclear clumps were found at several hyphal tips and sometimes in subapical regions. Partitioning of nuclear clusters between two branches were occasionally observed (Fig. 5C) in addition to single nuclei separated from clusters. Both events probably account for the presence of multiple nuclear clumps in the older Ag*dhc1*Δ mycelia.

During development of our dynein mutants, lateral hyphal branches could form and elongate properly suggesting that nuclei concentrated at the tip can still support the growth of adjacent branches. However, lateral branches that were too far away from the nuclear clump stopped elongating and frequently lysed.

Microtubule network and actin organization in *Agdhc1* null mutants

Nuclear migration is a microtubule-based process in fungi (Oakley and Morris, 1980; Huffaker et al., 1988; Palmer et al., 1992). To find out whether microtubule organization is disturbed in the Ag*dhc1* null mutant, indirect tubulin immunofluorescence as well as DAPI staining were performed on formaldehyde-fixed cells (Fig. 6A-E). In wild-type hyphae where nuclei are uniformly distributed, long cytoplasmic microtubules are dispersed throughout most of the cytosol and positioned predominantly parallel to the axis of growth (Fig. 6A,B). A similar microtubule organization has already been described in other filamentous fungi (Oakley et al., 1990; Inoue et al., 1998; Minke et al., 1999a; Minke et al., 1999b). For most *A. gossypii* wild-type hyphae we observed 3-4 microtubule tracks. It is not clear whether these long cytoplasmic tracks represent single microtubules or microtubule bundles. It is also not clear whether nuclei are in contact with only one or with several microtubule tracks. Immunostaining of the *Agdhc1* null mutant (Fig. 6C-E) revealed the presence of long cytoplasmic microtubules starting at the basal region of the nuclear clump and extending for up to 90 μm (n=12) into anucleate hyphae (see Fig. 6C,E). The presence of cytoplasmic microtubules in the Ag*dhc1* null mutant indicates that the ability to generate

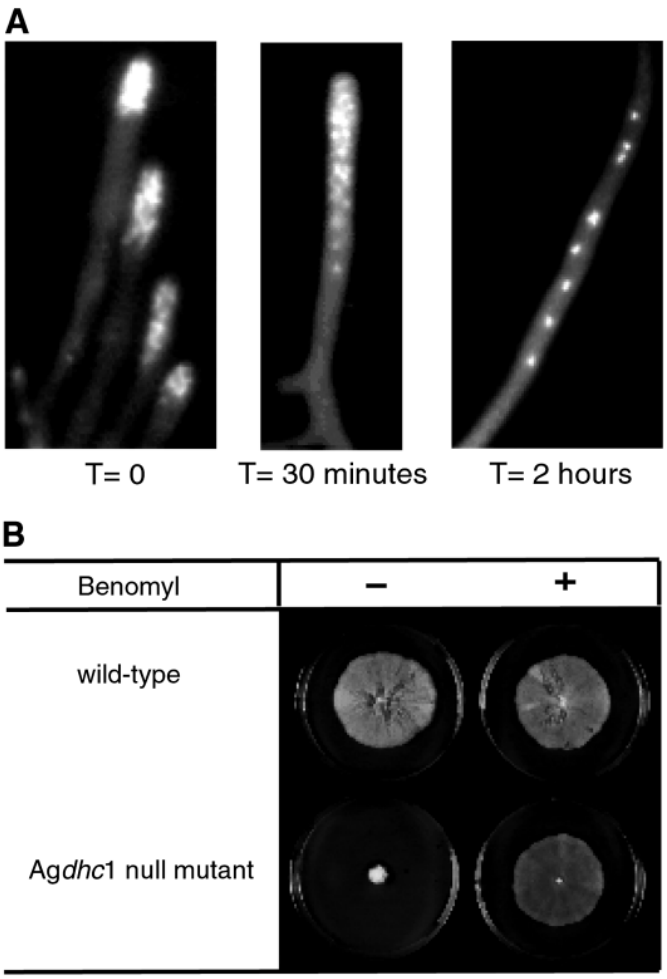

Fig. 7. Suppression of nuclear distribution and growth defects of Ag*dhc1* null mutant by benomyl. (A) DAPI staining of Ag*dhc1*Δ young hyphae before and after treatment with 33 μM benomyl. (B) Radial growth of wild type and Ag*dhc1* null mutant on AFM plates in the presence or absence of benomyl (33 μM). Plates were incubated 5 days at 30°C.

microtubule tracks is not lost in the absence of the dynein motor. We still observed 3-4 microtubule tracks permeating the cytosol which were often very close to each other and could only be resolved by deconvolution techniques. Compared to the *A. gossypii* wild type, the cytoplasmic microtubules observed in the Ag*dhc1*null mutant are more contorted as evident from quantitative evaluations. The average length of MT tracks in wild-type and Ag*dhc1* mutant were measured in consecutive hyphal segments of 12 μm length and were found to be 12.45 μm (s.d.=0.31; n=30) and 14.03 μm (s.d.=1.39; n=30), respectively.

In filamentous fungi, actin is mostly concentrated at the growing apex and is thought to be involved in the transport of secretory vesicles required for hyphal tip extension (Heath, 1990). Because hyphal tips carrying a cluster of up to 50 nuclei were still able to grow, we were wondering how such compartments organize actin. Therefore we stained *A. gossypii* wild-type and Ag*dhc1*Δ strains with rhodamine-phalloidine and DAPI. In wild-type hyphae actin is organized in cables and cortical patches dispersed along the hyphal cortex with an enrichment of patches at hyphal tips (Fig. 6F,G). Hyphal tip compartments of Ag*dhc1*Δ with nuclear clusters were found to form a similar actin cytoskeleton (Fig. 6H-L). We also observed actin cables and patches in nuclei-free hyphae including branches (Fig. 6J-L). We conclude from these data that the *A. gossypii* dynein motor is not required for the organization of actin and that a high density of nuclei in tip compartments does not prevent formation of an actin cytoskeleton.

Effect of a microtubule-destabilizing drug on *Agdhc1* null mutants

As shown above, immunostaining of *Agdhc1* revealed the presence of long cytoplasmic microtubules emanating from the basal region of each nuclear cluster. We wanted to determine whether a microtubule-destabilizing drug such as benomyl could have an effect on the distribution of nuclei in the *Agdhc1*Δ hyphae. Therefore we grew *Agdhc1*Δ young mycelia exhibiting nuclear clusters at the hyphal tips in AFM liquid medium containing different concentrations of benomyl. Aliquots were stained with DAPI and analysed by microscopy. Results obtained with 33 μM benomyl are presented in Fig. 7A. After 30 minutes of incubation at 30°C we observed a dissolution of the nuclear cluster at the hyphal tip concomitant with a fragmentation of the cytoplasmic microtubules. Two hours after addition of benomyl the nuclei were redistributed more or less regularly within the hyphae. To determine whether this nuclear redistribution correlated with a recovery of growth, we inoculated small pieces of *Agdhc1*Δ and wild-type mycelia on 33 μM benomyl-containing AFM plates (Fig. 7B). The wild-type growth was apparently not affected by the drug treatment except that the mycelium appeared thinner. In addition, we noticed a slight decrease in sporulation efficiency in the benomyl-treated *A. gossypii* wild type. In contrast, the growth of the *Agdhc1*null mutants was considerably improved. After 5 days incubation at 30°C the Ag*dhc1* null mutant succeeded in forming a round colony whose diameter was equivalent to that of the wild type. This growth improvement in the presence of benomyl, however, did not lead to spore production. To exclude the possibility that the positive effects on nuclear distribution and growth were due to the presence of DMSO, used as a solvent, *Agdhc*1 null mutants were incubated in the presence of the organic solvent alone. No change in nuclear distribution or growth was observed.

We were also interested in following spore germination in the presence of 33 μM benomyl. Germinating spores showed a wild-type-like nuclear distribution with dynamics as described in Fig. 5A. In older hyphae we did not observed any nuclear clustering and nuclei were more or less evenly distributed over the entire length of the hyphae. This demonstrates that benomyl is able to effectively compensate for the loss of the cytoplasmic dynein motor with respect to nuclear distribution. The same positive effect was also observed in the presence of 8 μM nocodazole (data not shown). However, suppressions of nuclear distribution and growth defects were not as complete as those observed with benomyl.

DISCUSSION

Nuclear movement and positioning in filamentous fungi have

been proposed to be the result of different opposing forces acting on each nucleus (McKerracher and Heath, 1986; Plamann et al., 1994). During hyphal extension a unidirectional movement of nuclei towards the tip could be achieved when the tip-directed force is stronger than the opposing retrograde force. Positioning of nuclei at specific locations would occur when such opposing forces reach an equilibrium.

Properties of nuclear migration in *A. gossypii*

Our in vivo study of nuclear migration in *A. gossypii* revealed a detailed picture of long range nuclear migration. The frequent and apparently independent oscillations of nuclei confirm the existence of opposing forces of variable strength acting on each nucleus. The net movement of nuclei towards the growing tip is most likely achieved when the tip-directed force is on average stronger than the retrograde force and when this difference is controlled by the hyphal tip extension rate. Whether such nuclear oscillations are also common in other filamentous fungi is not known. A similar time-lapse study on nuclear migration in *A. nidulans* could not reveal oscillatory motion of nuclei (Suelmann et al., 1997). However, this could have been due to limited time resolution. The abolition of the oscillations by a microtubule-destabilizing drug such as nocodazole, at a concentration that still allows colony growth, indicates that these opposing forces are generated either by the intrinsic dynamics of microtubules alone or in connection with microtubule-based motor proteins. Using video microscopy we could show that these non-oscillating nuclei were still able to move towards the tip. Such movement may be caused by cytoplasmic streaming or by a force that remains to be identified.

Dynamics of nuclear division in *A. gossypii*

In vivo studies of nuclear and spindle dynamics in the budding yeast *S. cerevisiae* revealed two phases for anaphase B, a rapid initial elongation of the spindle followed by a period of slower elongation (Kahana et al., 1995; Yeh et al., 1995; Straight et al., 1997). To perform similar kinetic measurements in *A. gossypii* we first tried to construct a strain with functional GFP-labelled microtubules. However, despite much effort this has so far unsuccessful. In a recent study with *S. cerevisiae* it has been shown that the orientation and elongation of the mitotic spindle can be inferred from the behaviour of the two dividing chromosomal masses labelled with histone-GFP (Hoepfner et al., 2000). Therefore we carefully measured, in *A. gossypii*, the separation kinetics of the two daughter DNA masses labelled with GFP. This quantification with a time resolution of one picture every minute revealed uniphasic kinetics of nuclear division. The measured 0.64 μm/minute (s.d.=0.08; n=7) elongation rate is in the same range as the fast elongation rate observed for haploid *S. cerevisiae* (Table 1). Also, the maximal elongation to around 9 μm is very similar in both organisms. The main difference in mitosis is that nuclear separation requires less time in *A. gossypii* than in *S. cerevisiae* (Table 1).

In the yeast *S. cerevisiae* two molecular motors have been found to be involved in the two distinct phases of nuclear elongation (Straight et al., 1998): the CIN8 motor is required for the rapid phase of mitotic spindle elongation and the KIP1 motor for the slower phase. We have found homologs to both motors in *A. gossypii*. Their contribution to nuclear separation remains to be elucidated.

Microtubules and timing of mitosis

Hyphae of filamentous ascomycetes typically contain several cytoplasmic microtubule tracks often located near the hyphal cortex but also passing through the middle of the hyphal tubes. In *A. nidulans* four to six microtubule tracks have been observed (Oakley et al., 1990; Fischer, 1999). For *N. crassa* the existence of two classes of cytoplasmic microtubules has been reported, one with no obvious association with nuclei and the other connecting adjacent nuclei via astral microtubules emanating from their spindle pole bodies (Minke et al., 1999a). In *A. gossypii* we observed three to four cytoplasmic microtubule tracks which extended close to the hyphal tip. A distinction between nuclei-associated and non-associated microtubules was however not possible. With respect to the

Table 1. Parameters of nuclear division in *S. cerevisiae* (S.c.) and *A. gossypii* (A.g.)

Strains	Unelongated spindle (μm)	Breakdown length (μm)	Fast spindle elongation (μm/min)	Slow spindle elongation (μm/min)	Anaphase duration (min)	Reference and microscopy method
S.c. diploid S.c. haploid	1.5-2.0	8-12	1.08±0.31	0.3-0.4	25-35	Yeh, E. et al., 1995. DE and VE-DIC light microscopy
S.c. diploid	n.d.	appr. 10	1.48±0.11	0.69±0.14	15-30	Kahana, J. A. et al., 1995. Fluorescence microscopy with GFP-labelled SPB
S.c. haploid	1.5-2.0	9.52±0.49	0.54±0.02	0.21±0.01	26.6±1.6	Straight, A. F. et al., 1997. Fluorescence microscopy with GFP-labelled spindle
S.c. haploid*	2.02±0.11	10.50±0.49	0.73±0.07	0.26±0.02	21.8±2.8	Hoepfner, D., unpublished. Fluorescence microscopy with GFP-labelled spindle
A.g. haploid‡	2.23±0.21	8-9	0.64±0.08	n.a	10-12	This study. Fluorescence microscopy with GFP-labelled histone

*These measurements were performed with the same microscopic setting used for the *A. gossypii* investigation.

‡In these measurements we assume that the dynamics of separation of the two daughter nuclear masses is similar to spindle dynamics, that the end-to-end distance of the non-divided nucleus is equivalent to the unelongated spindle length, and that the maximal end-to-end distance of the connected daughter nuclear masses corresponds to the spindle breakdown length.

maintenance of these long microtubule tracks important differences have been reported. For example in hyphal compartments of *A. nidulans* the cytoplasmic microtubules disassemble prior to the synchronous mitosis of nuclei (Oakley et al., 1990). This is different from *N. crassa* where nuclei in hyphal tip compartments undergo asynchronous mitosis, and disassembly of microtubule tracks in compartments with dividing nuclei has not been observed (Minke et al., 1999a). Nuclear divisions in *A. gossypii* are also asynchronous and in all hyphal tip compartments analysed we observed extended microtubule tracks. Moreover oscillations of interphase nuclei continued when adjacent nuclei underwent mitosis implying the existence of intact microtubule tracks in compartments with dividing nuclei. Altogether these studies indicate that microtubule-dependent nuclear movement in filamentous ascomycetes does not seem to follow the same rules.

Possible function of cytoplasmic dynein in *A. gossypii*

In order to study *A. gossypii* strains lacking DHC1 activity we deleted the entire 12.2 kb Ag*DHC*1 ORF. This deletion resulted in the formation of nuclear clusters at the tip of *A. gossypii* hyphae leaving behind anucleate hyphal compartments. This suggests that a major force for nuclear movement was lost. The simplest explanation is that dynein in *A. gossypii* is counteracting the force that is directing the nuclei towards the tip. This result is in contrast to those obtained in *A. nidulans*, where the inactivation of dynein causes retention of nuclei in the germ bubble generating nuclei-free germ tubes (Xiang et al., 1994; Xiang et al., 1995). Moreover, inactivation of the dynein heavy chain in *N. crassa* and *N. haematococca* by a ts mutation or by disruption of the motor domain respectively, gave rise to slowly growing mycelia containing many nuclear clusters. The clusters were distributed throughout the hyphae but were lacking in all hyphal tip regions (Plamann et al., 1994; Inoue et al., 1998). These data suggest that the dynein motor in these three filamentous fungi is required to move the nuclei towards the tip. Therefore, the loss of the dynein motor has opposite effects on nuclear migration in *A. gossypii* compared to *A. nidulans*, *N. crassa* and *N. haematococca*.

The nature of the force directed to the tip is still unknown in *A. gossypii*. However, we showed that nocodazole, a microtubule-destabilizing drug, abolishes back and forth motion of nuclei in wild-type hyphae. Therefore, the force that is directing nuclei towards the tip also seems to depend on microtubules. We have began to look for candidates for such a force. In *S. cerevisiae* for example, in addition to dynein, the three kinesin motors KIP2, KIP3, KAR3 were shown to be involved in nuclear movement (DeZwaan et al., 1997; Saunders et al., 1997; Miller et al., 1998; Cottingham et al., 1999). In *A. gossypii* we have identified and deleted genes with homology to the KIP2, KIP3 and KAR3 motors. None of these deletions led to nuclear clusters distant from tips or to a nonuniform nuclear distribution with anucleate hyphal tips (C. Alberti-Segui, unpublished data). Therefore, we believe that either microtubules alone or together with more than one microtubule-based motor support the movement of nuclei towards the tip.

We observed a redistribution of nuclei and a regain of a wild-type like growth in the Ag*dhc1* null mutant in the presence of benomyl, a microtubule-destabilizing drug. This is most likely achieved by destabilization of the long cytoplasmic microtubules extending from the basal end of the nuclear cluster into anucleate regions and by the concomitant alleviation of the basis for the tip-directed force. Interestingly, in dynein mutants of *A. nidulans* benomyl treatment also leads to a redistribution of nuclei (Willins et al., 1995), suggesting that in both organisms the nuclear clumping can be suppressed by microtubule destabilization. The clear difference between the phenotypes of dynein inactivation in *A. gossypii* and *A. nidulans* suggests that either the mechanisms of nuclear migration is different or that the basic nuclear transport machinery is very similar, but that cytoplasmic microtubules are differently oriented in these two systems. Therefore, the elucidation of the polarity and dynamics of cytoplasmic microtubules is an important prerequisite to understanding how nuclear migration is achieved in these filamentous fungi.

We thank all members of the *Ashbya* team for numerous discussions and constant encouragement. We acknowledge the supporting interest of Gero Steinberg in this work and his comments about the manuscript. We also thank Tom Gaffney, Sylvia Voegeli, Rainer Pöhlmann and Roger Schmidt for help in sequencing the complete *A. gossypii* dynein heavy chain gene. We wish to thank R. Sütterlin for providing secondary antibodies used in the microtubule immunostaining. The work was supported by funds of the University of Basel, Novartis Agribusiness Biotechnology Research Inc. and the Swiss National Science Foundation (Grant 3100-055941.98).

REFERENCES

Altmann-Jöhl, R. (1996). *Comparative gene and genome analysis in the filamentous fungus* Ashbya gossypii *and the yeast* Saccharomyces cerevisiae. Ph. D. thesis, Biozentrum, University of Basel, Switzerland.

Ashby, S. F. and Nowell, W. (1926). The fungi of stigmatomycosis. *Ann. Bot.* **40**, 69-84.

Ayad-Durieux, Y., Knechtle, P., Goff, S., Dietrich, F. and Philippsen, P. (2000). A PAK-like protein kinase is required for maturation of young hyphae and septation in the filamentous ascomycete *Ashbya gossypii*. *J. Cell Sci.* **113**, 4563-4575.

Beckwith, S. M., Roghi, C. H. and Morris, N. R. (1995). The genetics of nuclear migration in fungi. *Genet. Eng.* **17**, 165-180.

Carminati, J. L. and Stearns, T. (1997). Microtubules orient the mitotic spindle in yeast through dynein- dependent interactions with the cell cortex. *J. Cell Biol.* **138**, 629-641.

Cottingham, F. R. and Hoyt, M. A. (1997). Mitotic spindle positioning in *Saccharomyces cerevisiae* is accomplished by antagonistically acting microtubule motor proteins. *J. Cell Biol.* **138**, 1041-1053.

Cottingham, F. R., Gheber, L., Miller, D. and Hoyt, M. A. (1999). Novel roles for *Saccharomyces cerevisiae* mitotic spindle motors. *J. Cell Biol.* **147**, 335-349.

DeZwaan, T. M., Ellingson, E., Pellman, D. and Roof, D. M. (1997). Kinesin-related KIP3 of *Saccharomyces cerevisiae* is required for a distinct step in nuclear migration. *J. Cell Biol.* **138**, 1023-1040.

Eshel, D., Urrestarazu, L. A., Vissers, S., Jauniaux, J. C., van Vliet-Reedijk, J. C., Planta, R. J. and Gibbons, I. R. (1993). Cytoplasmic dynein is required for normal nuclear segregation in yeast. *Proc. Natl. Acad. Sci. USA* **90**, 11172-11176.

Fischer, R. (1999). Nuclear movement in filamentous fungi. *FEMS Microbiol. Rev.* **23**, 39-68.

Gee, M. A., Heuser, J. E. and Vallee, R. B. (1997). An extended microtubule-binding structure within the dynein motor domain. *Nature* **390**, 636-639.

Gordon, D., Abajian, C. and Green, P. (1998). Consed: a graphical tool for sequence finishing. *Genome Res.* **8**, 195-202.

Heath, I. B. (1990). The roles of actin in tip growth of fungi. *Int. Rev. Cytol.* **123**, 95-127.

Heim, R., Cubitt, A. B. and Tsien, R. Y. (1995). Improved green fluorescence. *Nature* **373**, 663-664.

Hildebrandt, E. R. and Hoyt, M. A. (2000). Mitotic motors in Saccharomyces cerevisiae. *Biochim. Biophys. Acta* **1496**, 99-116.

Hirozumi, K., Nakajima, H., Machida, M., Yamaguchi, M., Takeo, K. and Kitamoto, K. (1999). Cloning and characterization of a gene (arpA) from Aspergillus oryzae encoding an actin-related protein required for normal nuclear distribution and morphology of conidiophores. *Mol. Gen. Genet.* **262**, 758-767.

Hoepfner, D., Brachat, A. and Philippsen, P. (2000). Time-lapse video microscopy analysis reveals astral microtubule detachment in the yeast spindle pole mutant cnm67. *Mol. Biol. Cell* **11**, 1197-1211.

Huffaker, T. C., Thomas, J. H. and Botstein, D. (1988). Diverse effects of beta-tubulin mutations on microtubule formation and function. *J. Cell Biol.* **106**, 1997-2010.

Inoue, S., Turgeon, B. G., Yoder, O. C. and Aist, J. R. (1998). Role of fungal dynein in hyphal growth, microtubule organization, spindle pole body motility and nuclear migration. *J. Cell Sci.* **111**, 1555-1566.

Kahana, J. A., Schnapp, B. J. and Silver, P. A. (1995). Kinetics of spindle pole body separation in budding yeast. *Proc. Natl. Acad. Sci. USA* **92**, 9707-9711.

Koonce, M. P. (1997). Identification of a microtubule-binding domain in a cytoplasmic dynein heavy chain. *J. Biol. Chem.* **272**, 19714-19718.

Koonce, M. P. and Tikhonenko, I. (2000). Functional Elements within the Dynein Microtubule-binding Domain. *Mol. Biol. Cell* **11**, 523-529.

Li, Y. Y., Yeh, E., Hays, T. and Bloom, K. (1993). Disruption of mitotic spindle orientation in a yeast dynein mutant. *Proc. Natl. Acad. Sci. USA* **90**, 10096-10100.

Maeting, I., Schmidt, G., Sahm, H., Revuelta, J. L., Stierhof, Y. D. and Stahmann, K. P. (1999). Isocitrate lyase of Ashbya gossypii–transcriptional regulation and peroxisomal localization. *FEBS Lett.* **444**, 15-21.

McKerracher, L. J. and Heath, I. B. (1986). Fungal nuclear behaviour analyzed by ultraviolet microbeam irradiation. *Cell Motil. Cytoskeleton* **6**, 35-47.

Meluh, P. B. and Rose, M. D. (1990). KAR3, a kinesin-related gene required for yeast nuclear fusion [published erratum appears in *Cell* 1990 May 4;61(3):548]. *Cell* **60**, 1029-1041.

Miller, R. K., Heller, K. K., Frisen, L., Wallack, D. L., Loayza, D., Gammie, A. E. and Rose, M. D. (1998). The kinesin-related proteins, Kip2p and Kip3p, function differently in nuclear migration in yeast. *Mol. Biol. Cell* **9**, 2051-2068.

Minke, P. F., Lee, I. H. and Plamann, M. (1999a). Microscopic analysis of neurospora ropy mutants defective in nuclear distribution. *Fungal Genet. Biol.* **28**, 55-67.

Minke, P. F., Lee, I. H., Tinsley, J. H., Bruno, K. S. and Plamann, M. (1999b). Neurospora crassa ro-10 and ro-11 genes encode novel proteins required for nuclear distribution. *Mol. Microbiol.* **32**, 1065-1076.

Mohr, C. (1997). *Genetic engineering of the filamentous fungus Ashbya gossypii: construction of a genomic library, isolation of genes for beta-isopropylmalate-dehydrogenase (LEU2) and a protein kinase (APK1) by heterologous complementation, and characterization of non-reverting mutants.* PhD thesis, Biozentrum, University of Basel, Switzerland.

Morris, N. R., Xiang, X. and Beckwith, S. M. (1995). Nuclear migration advances in fungi. *Trends Cell Biol.* **5**, 278-282.

Oakley, B. R. and Morris, N. R. (1980). Nuclear movement is beta–tubulin-dependent in Aspergillus nidulans. *Cell* **19**, 255-262.

Oakley, B. R., Oakley, C. E., Yoon, Y. and Jung, M. K. (1990). Gamma-tubulin is a component of the spindle pole body that is essential for microtubule function in Aspergillus nidulans. *Cell* **61**, 1289-1301.

Palmer, R. E., Sullivan, D. S., Huffaker, T. and Koshland, D. (1992). Role of astral microtubules and actin in spindle orientation and migration in the budding yeast, Saccharomyces cerevisiae. *J. Cell Biol.* **119**, 583-593.

Plamann, M., Minke, P. F., Tinsley, J. H. and Bruno, K. S. (1994). Cytoplasmic dynein and actin-related protein Arp1 are required for normal nuclear distribution in filamentous fungi. *J. Cell Biol.* **127**, 139-149.

Saunders, W., Hornack, D., Lengyel, V. and Deng, C. (1997). The Saccharomyces cerevisiae kinesin-related motor Kar3p acts at preanaphase spindle poles to limit the number and length of cytoplasmic microtubules. *J. Cell Biol.* **137**, 417-431.

Sikorski, R. S. and Hieter, P. (1989). A system of shuttle vectors and yeast host strains designed for efficient manipulation of DNA in Saccharomyces cerevisiae. *Genetics* **122**, 19-27.

Steiner, S., Wendland, J., Wright, M. C. and Philippsen, P. (1995). Homologous recombination as the main mechanism for DNA integration and cause of rearrangements in the filamentous ascomycete Ashbya gossypii. *Genetics* **140**, 973-987.

Suelmann, R., Sievers, N. and Fischer, R. (1997). Nuclear traffic in fungal hyphae: in vivo study of nuclear migration and positioning in Aspergillus nidulans. *Mol. Microbiol.* **25**, 757-769.

Straight, A. F., Marshall, W. F., Sedat, J. W. and Murray, A. W. (1997). Mitosis in living budding yeast: anaphase A but no metaphase plate. *Science* **277**, 574-578.

Straight, A. F., J. W. Sedat and Murray, A. W. (1998). Time-lapse microscopy reveals unique roles for kinesins during anaphase in budding yeast. *J. Cell Biol.* **143**,687-694.

Thierry, A., Fairhead, C. and Dujon, B. (1990). The complete sequence of the 8.2 kb segment left of MAT on chromosome III reveals five ORFs, including a gene for a yeast ribokinase. *Yeast* **6**, 521-534.

Tinsley, J. H., Minke, P. F., Bruno, K. S. and Plamann, M. (1996). p150Glued, the largest subunit of the dynactin complex, is nonessential in Neurospora but required for nuclear distribution. *Mol. Biol. Cell* **7**, 731-742.

Wach, A., Brachat, A., Alberti-Segui, C., Rebischung, C. and Philippsen, P. (1997). Heterologous HIS3 marker and GFP reporter modules for PCR-targeting in Saccharomyces cerevisiae. *Yeast* **13**, 1065-1075.

Wendland, J., Ayad-Durieux, Y., Knechtle, P., Rebischung, C. and Philippsen, P. (2000). PCR-based gene targeting in the filamentous fungus Ashbya gossypii. *Gene* **242**, 381-391.

Wendland, J. and Philippsen, P. (2000). Determination of cell polarity in germinated spores and hyphal tips of the filamentous ascomycete ashbya gossypii requires a rhoGAP homolog. *J. Cell. Sci.* **113**, 1611-1621.

Willins, D. A., Xiang, X. and Morris, N. R. (1995). An alpha tubulin mutation suppresses nuclear migration mutations in Aspergillus nidulans. *Genetics* **141**, 1287-1298.

Womble, D. D. (2000). GCG: The Wisconsin Package of sequence analysis programs. *Methods Mol. Biol.* **132**, 3-22.

Wright, M. C. and Philippsen, P. (1991). Replicative transformation of the filamentous fungus Ashbya gossypii with plasmids containing Saccharomyces cerevisiae ARS elements. *Gene* **109**, 99-105.

Xiang, X., Beckwith, S. M. and Morris, N. R. (1994). Cytoplasmic dynein is involved in nuclear migration in Aspergillus nidulans. *Proc. Natl. Acad. Sci. USA* **91**, 2100-2104.

Xiang, X., Roghi, C. and Morris, N. R. (1995). Characterization and localization of the cytoplasmic dynein heavy chain in Aspergillus nidulans. *Proc. Natl. Acad. Sci. USA* **92**, 9890-9894.

Yeh, E., Skibbens, R. V., Cheng, J. W., Salmon, E. D. and Bloom, K. (1995). Spindle dynamics and cell cycle regulation of dynein in the budding yeast, Saccharomyces cerevisiae. *J. Cell Biol.* **130**, 687-700.